

The Minimum Halo Mass for Star Formation at $z = 6–8$

Kristian Finlator^{1,8,11}, Moire K. M. Prescott^{1,8}, B. D. Oppenheimer⁴, Romeel Davé^{5,6,7}, E. Zackrisson³, R. C. Livermore¹⁰, S. L. Finkelstein¹⁰, Robert Thompson⁹, Shuiyao Huang²

¹ *New Mexico State University, Las Cruces, NM, USA*

² *University of Massachusetts, Amherst, MA, USA*

³ *Department of Physics and Astronomy, Uppsala University, 751 20 Uppsala, Sweden*

⁴ *CASA, Department of Astrophysical and Planetary Sciences, University of Colorado, 389-UCB, Boulder, CO 80309, USA*

⁵ *University of the Western Cape, Bellville, Cape Town 7535, South Africa*

⁶ *South African Astronomical Observatories, Observatory, Cape Town 7525, South Africa*

⁷ *African Institute for Mathematical Sciences, Muizenberg, Cape Town 7545, South Africa*

⁸ *Dark Cosmology Centre, Niels Bohr Institute, University of Copenhagen, Copenhagen, Denmark*

⁹ *NCSA, University of Illinois, Urbana-Champaign, IL 61820*

¹⁰ *The University of Texas at Austin, 2515 Speedway, Stop C1400, Austin, TX 78712, USA*

¹¹ *finlator@nmsu.edu*

22 September 2016

ABSTRACT

Recent analysis of strongly-lensed sources in the Hubble Frontier Fields indicates that the rest-frame UV luminosity function of galaxies at $z = 6–8$ rises as a power law down to $M_{UV} = -15$, and possibly as faint as -12.5 . We use predictions from a cosmological radiation hydrodynamic simulation to map these luminosities onto physical space, constraining the minimum dark matter halo mass and stellar mass that the Frontier Fields probe. While previously-published theoretical studies have suggested or assumed that early star formation was suppressed in halos less massive than $10^9–10^{11}M_{\odot}$, we find that recent observations demand vigorous star formation in halos at least as massive as $(3.1, 5.6, 10.5) \times 10^9 M_{\odot}$ at $z = (6, 7, 8)$. Likewise, we find that Frontier Fields observations probe down to stellar masses of $(8.1, 18, 32) \times 10^6 M_{\odot}$; that is, they are observing the likely progenitors of analogues to Local Group dwarfs such as Pegasus and M32. Our simulations yield somewhat different constraints than two complementary models that have been invoked in similar analyses, emphasizing the need for further observational constraints on the galaxy-halo connection.

Key words: cosmology: theory — galaxies: high-redshift — galaxies: formation — galaxies: evolution — galaxies: haloes

1 INTRODUCTION

A key question regarding the way in which dark matter halos grow galaxies is the minimum mass of a dark matter halo M_{\min} that can both retain its gas and condense it efficiently onto a galaxy. Locally, this question is central to both the “missing satellites” and the “too big to fail” problems (Klypin et al. 1999; Boylan-Kolchin et al. 2011). In the context of the reionization epoch ($z \geq 6$), it arises because of the possible role of faint galaxies in driving the growth of the nascent ultraviolet ionizing background (UVB): the steep observed slope of the UV luminosity function’s (LF) faint end gives rise to a luminosity density that diverges if integrated to arbitrarily faint luminosities. Hence faint galaxies could well have driven reionization and dominated the UVB, but only if the limiting luminosity out to which the LF continues as a power law

is quite faint (Robertson et al. 2013; Finkelstein et al. 2012; Kuhlen & Faucher-Giguère 2012). As a minimum luminosity would imply a minimum halo mass, measurements of the former can be invoked as a constraint on the latter.

This, in turn, would constrain a number of physical processes that can regulate gas cooling, star formation, and feedback in low-mass halos. For example, “Jeans Filtering” prevents gas from being accreted by dark matter halos whose virial temperature is less than the (appropriately time-averaged) temperature of the ambient intergalactic medium (IGM; Efstathiou 1992; Quinn et al. 1996; Gnedin 2000; Okamoto et al. 2008). While the effect is expected to play a role even in the absence of reionization (Naoz et al. 2009), idealized simulations predict that the latent heat from photoionization completely halts gas accretion in halos with circular velocities V_{circ} below 30 km s^{-1} but is negligible

2 The Minimum Mass for Star Formation at $z = 6-8$

for $V_{\text{circ}} > 75 \text{ km s}^{-1}$ (Thouly & Weinberg 1996). Similarly, three-dimensional simulations indicate that it suppresses the gas reservoirs of halos less massive than $3 \times 10^8 M_{\odot}$ ($V_{\text{circ}} < 26 \text{ km s}^{-1}$) at $z = 6$ (Okamoto et al. 2008; Finlator et al. 2012). This idea has motivated extended reionization models in which star formation is assumed not to occur in reionized regions in halos less massive than $1-2 \times 10^9 M_{\odot}$ (Iliev et al. 2007; Alvarez et al. 2012; Mesinger & Dijkstra 2008). Building further on this idea, Bouché et al. (2010) proposed that gas in halos less massive than $10^{11} M_{\odot}$ does not accrete efficiently onto the central galaxy owing to photoionization feedback from hot stars at $z > 6$. They showed that this assumption naturally allows a simple model to reproduce measurements of galaxy downsizing at $z \leq 2$. Note that these theoretical studies invoke similar physics but assume threshold masses that vary by two orders of magnitude, clearly motivating the need for observational constraints.

An additional effect that is related to Jeans suppression is photoevaporation: During the reionization epoch, ionization fronts likely evaporated gas that was bound to minihalos ($< 10^{7-8} M_{\odot}$; Shapiro et al. 2004), suppressing further star formation below this mass range. Even in the absence of a UVB, halos whose virial temperature is less than 10^4 K cannot cool and condense their gas through collisional excitation of neutral hydrogen; they are dependent on molecular hydrogen formation cooling, which is relatively inefficient. These effects have been modeled in high-resolution, ab-initio numerical simulations, leading to predictions that the reionization-epoch LF flattens for luminosities $M_{\text{UV}} < -12$ (Wise et al. 2014).

Another source of suppression is galactic outflows, which are closely associated with vigorous star formation (Veilleux et al. 2005). A variety of theoretical models indicate that outflows are more efficient at removing gas from galaxies and suppressing their growth when they live in low-mass halos (Dekel & Silk 1986; Heckman 2002; Murray et al. 2005; Muratov et al. 2015; Christensen et al. 2016). They may even introduce a characteristic scale below which suppression is particularly efficient (Dekel & Silk 1986; Muratov et al. 2015).

Finally, recent models in which the local star formation rate density is computed from the local density of molecular hydrogen (as opposed to the total gas density) predict that galaxy growth is suppressed in dark matter halos less massive than $10^{10} M_{\odot}$ (Krumholz & Dekel 2012; Kuhlen et al. 2012). If true, then the $z = 6$ UV LF is expected to turn over at an absolute magnitude of ≈ -15 (Jaacks et al. 2013).

Given the importance of the high-redshift UV LF as a probe of activity in low-mass halos, multiple techniques for interpreting it have been developed. One method involves assuming that local group dwarf galaxies are representative of the high-redshift population and using spatially-resolved star formation histories to infer the abundance and activity in their progenitor population. Weisz et al. (2014b) used this approach to argue that the intrinsic $z > 5$ LF grows without a turnover to at least $M_{\text{UV}} = -5$. However, a subsequent analysis found that it may flatten for $M_{\text{UV}} > -13$ (Boylan-Kolchin et al. 2015; see also Boylan-Kolchin et al. 2014), in better agreement with predictions from ab-initio simulations (for example, Wise et al. 2014).

More directly, a number of groups have used imaging from the Hubble Frontier Fields to trace the UV LF out

to unprecedented depths (Atek et al. 2015; Ishigaki et al. 2015, 2016; Laporte et al. 2016; Livermore et al. 2016; Bouwens et al. 2016). The deepest measurements are reported by Livermore et al. (2016), who use a wavelet decomposition approach to remove foreground light from galaxies associated with the lensing clusters. This allows them to identify many more faint systems than had previously been detected. They find that the UV LF is inconsistent with a turnover at $M < -12.5$ at $z = 6$, with weaker constraints at higher redshifts.

What do the Livermore et al. (2016) measurements imply for galaxy growth in low-mass halos? Qualitatively, the finding that the slopes of the dark matter halo mass function at low masses and the UV LF at faint luminosities are similar (≈ -2 in both cases) implies that galaxy luminosity varies nearly linearly with the host halo’s mass down to the faintest detected systems. Moreover, evidence for a minimum halo mass below which gas accretion and star formation are inefficient has not yet been detected. Instead, the Livermore et al. (2016) data place an upper limit on M_{min} . This limit constrains the efficiency of physical effects that limit star formation in low-mass halos. Additionally, it informs simplified reionization models that “paint” luminosities directly onto dark matter halos: they are disfavored if they invoke significant suppression where it is not observed.

A simple way to derive this limit is to impose a minimum halo mass cutoff on a galaxy formation model and ask how large that cutoff may be made before it introduces conflict with the observed LF. While similar comparisons have been undertaken before (Muñoz & Loeb 2011; Castellano et al. 2016), the arrival of significantly deeper measurements motivates us to revisit the problem. Additionally, galaxy formation models are now able to address a broader range of observables simultaneously than before. In particular, Finlator et al. (2016) discussed a numerical hydrodynamic + continuum radiation transport model that reproduces both the observed UV LF and the abundance of low-ionization metal absorbers (Finlator et al. 2016). Moreover, it predicts an integrated optical depth to Thomson scattering of 0.059, in excellent agreement with the most recent constraints from the cosmic microwave background (Planck Collaboration 2016a,b). In short, this model yields favorable agreement with observations of galaxies, absorbers, and a spatially-inhomogeneous reionization history simultaneously, opening up the possibility of understanding how these observables relate to one another. It is therefore a particularly well-tested framework for interpreting the observed LF.

In this work, we use this simulation to interpret the constraints reported by Livermore et al. (2016) as an upper limit on M_{min} at $z > 6-8$, and on the lowest stellar mass of the galaxies that have been observed at this epoch. In Section 2, we review our simulations. In Section 3, we present our results. In Section 4, we discuss their implications and compare to previous work. In Section 5, we summarize.

2 SIMULATION AND ANALYSIS

We ran our cosmological radiation hydrodynamic simulation using a custom version of GADGET-3 (Springel 2005).

We previously presented this simulation in Finlator et al. (2016); the reader is referred to that work and to Section 2 of Finlator et al. (2015) for details of the physical treatments. Briefly, we discretize the mass in a periodic, cubical volume of comoving length $7.5h^{-1}\text{Mpc}$ into 2×320^3 dark matter and gas resolution elements and the radiation field into a regular spatial grid of 40^3 voxels and 16 independent frequency bins. Gas whose proper density exceeds 0.13 cm^{-3} forms stars via a subgrid multiphase treatment (Springel & Hernquist 2003). Star-forming gas is selectively added to galactic outflows following the “ezw” model (Davé et al. 2013). The ionizing emissivity is tied to the local star-forming gas particles’ metallicities and star formation rates using the YG-DRASIL (Zackrisson et al. 2011) spectral synthesis code. The assumed ionizing escape fraction depends both on redshift and halo mass (Finlator et al. 2015). The radiation field is evolved using a moment method, and we iterate at each timestep between the ionization and radiation solvers to obtain a consistent solution (Finlator et al. 2011, 2012).

We generate the initial conditions using an Eisenstein & Hu (1999) power spectrum at $z = 249$. We compute the initial gas ionization and temperature using RECFast (Wong et al. 2008). Our adopted cosmology is one in which $\Omega_M = 0.3$, $\Omega_\Lambda = 0.7$, $\Omega_b = 0.045$, $h = 0.7$, $\sigma_8 = 0.8$, and the index of the primordial power spectrum $n = 0.96$.

For each of our $z = 6, 7$, and 8 snapshots, we identify simulated galaxies using SKID¹ and compute their rest-frame 1500 \AA luminosities (in $\text{ergs sec}^{-1} \text{ Hz}^{-1}$) using version 2.3 of the Flexible Stellar Population Synthesis library (Conroy et al. 2009), interpolating to each star particle’s age and metallicity. The summed luminosities for each model galaxy are then expressed as absolute AB magnitudes. We neglect dust extinction because galaxies at $z \geq 6$ are observed to have relatively blue UV continua (Bouwens et al. 2014). In detail, our simulations do permit a small amount of dust; we will return to this possibility in our discussion of Figure 1 and consider it more closely in a future study.

We compute each galaxy’s host halo mass by growing a sphere about its center of mass until it encloses an overdensity that matches the expected overdensity of collapsed systems. A merging step re-assigns satellite galaxies to parent halos; we find that roughly 40% of galaxies are satellites.

Fundamentally, our study leverages the numerically predicted relationship between halo mass and UV luminosity, which we show in Figure 1. The model predicts significant scatter in this relationship: the host halo mass can vary by an order of magnitude even among centrals for $M_{\text{UV}} \leq -14$. Consequently, a given minimum luminosity corresponds to a lower minimum halo mass in our model than in a model in which the luminosity-halo mass relation is assumed to be scatter-free.

For context, we also compare our predicted halo mass-luminosity relation with two complementary analyses. Finkelstein et al. (2016) used an abundance-matching analysis to derive a relationship that has the same slope, but for which a typical halo is roughly one magnitude fainter (compare the circles with the dashed curve in Figure 1).

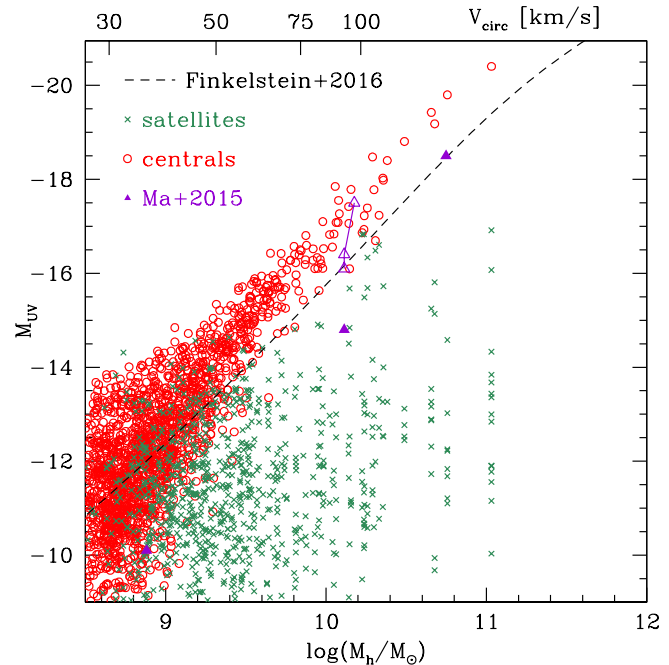


Figure 1. The simulated relationship between halo mass and UV luminosity at $z = 6$ both for centrals (red circles) and for satellites (green crosses). The scatter is quite significant, particularly for $M_{\text{UV}} > -17$.

This offset is somewhat surprising given that both relationships reproduce the observed UV LF. Assuming that the Finkelstein et al. (2016) fit is driven by bright galaxies, the inconsistency may confirm the suggestion that the simulation overproduces the bright end of the observed LF (Figure 2), though perhaps not as significantly as one might expect from Figure 1. The discrepancy cannot be resolved by adding dust to our models without rendering their UV continuum slopes too red: The predicted slopes β (where the flux $F_\lambda \propto \lambda^\beta$) for sources with $M_{\text{UV}} \approx -17 - -19$ are characteristically -2.5 , whereas observations indicate typical values of -2.3 (Bouwens et al. 2014). Adding enough dust to redden the predicted slopes into agreement with observations would dim them by ≤ 0.5 mag (Calzetti et al. 2000), eliminating no more than half of the gap between our predictions and Finkelstein et al. (2016). We have also verified that our simulation’s halo mass function agrees with analytical expectations to within 0.1 dex computed using HMF-CALC (Murray et al. 2013), so it is not the case that the model matches the observed LF by underproducing halos and overproducing stars within each halo. In any case, the disagreement at the fainter end, which is the subject of this work, is weaker owing to the large predicted scatter.

We also compare our predictions to those of Ma et al. (2015), who recently studied a small number of simulated galaxies with unprecedented numerical resolution and physical realism. Using a similar analysis to ours (including the decision to neglect dust), they find the relationship indicated by the solid magenta triangles. Their model predicts that galaxies are systematically 1–2 magnitudes fainter at a given halo mass than ours, although the lowest-mass halo lies within our model’s predicted scatter. Consistently with their Figure 4, we find that they predict overall fainter lumi-

¹ <http://www-hpcc.astro.washington.edu/tools/skid.html>

4 The Minimum Mass for Star Formation at $z=6-8$

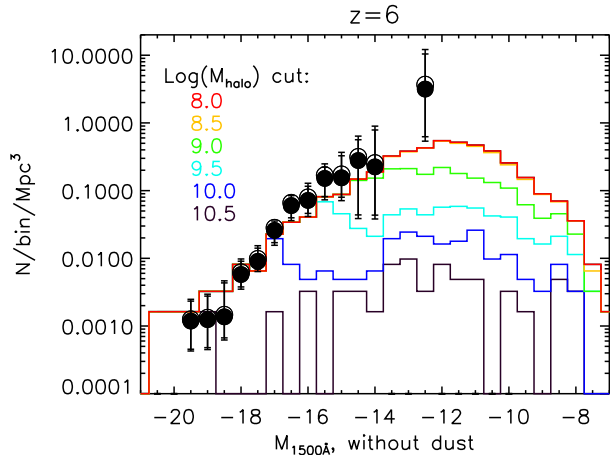


Figure 2. The simulated and observed luminosity functions at $z = 6$. As the minimum dark matter halo mass is increased, successively brighter galaxies are eliminated from the predicted LF. Measurements are from Livermore et al. (2016) and are shown both without (solid) and with (open) a correction for Eddington bias (see text).

nosities at given halo mass than is inferred from abundance-matching analyses. Ma et al. (2015) also re-simulated their $10^{10} M_{\odot}$ halo at eight times lower mass resolution using three different density thresholds for star formation, leading to generally brighter galaxies (open triangles) that are in much better agreement with our model and, ironically, empirical inferences (as represented here by Finkelstein et al. 2016). It is interesting to note that decreasing the mass resolution by a factor of 8 has a larger effect on M_{UV} than changing the threshold density for star formation by a factor of 100. This highlights the numerical challenge of modeling even individual galaxies at high redshift in a resolution-convergent way.

3 ANALYSIS AND RESULTS

In Figure 2, we illustrate our approach. With no tuning of parameters, the predicted dust-free LF is in excellent agreement with observations at $z = 6$ (red curve). We next impose a turnover in the LF by removing galaxies hosted by dark matter halos below a variable mass threshold M_c .² Increasing M_c moves the turnover to higher luminosity, weakening the agreement with observations.³ In the case of satellite galaxies, we remove them only if their parent halo mass exceeds the threshold. Qualitatively, this will lead to a *higher* (and hence more conservative) limit on M_{\min} than if we only considered the subhalo mass.

For a given cutoff halo mass M_c , we compute a $\chi^2(M_c)$

² For clarity, note that we use M_c to denote the model parameter and M_{\min} as the physically relevant minimum halo mass that we are trying to infer; that is, the value of M_c that is preferred by the data is a constraint on M_{\min} .

³ Imposing $M_c = 10^8 M_{\odot}$ (red curve in Figure 2) does not remove any star-forming halos in our simulation at $z \leq 8$ owing to photoionization heating, so it is equivalent to $M_c = 0$.

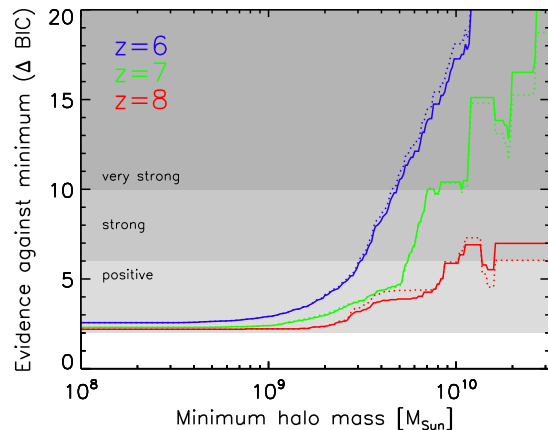


Figure 3. $\Delta\text{BIC}(M_c)$ versus M_c ; (blue, green, red) indicate the constraints at $z = (6, 7, 8)$. Solid/dashed curves indicate inferences without/with a correction to the data for Eddington Bias. The data, when compared with our model, provide strong evidence against models in which star formation is suppressed in halos less massive than $10^{9.5} M_{\odot}$ at $z = 6$, with weaker constraints resulting at higher redshifts.

statistic that quantifies the agreement between the predicted and observed LFs:

$$\chi^2(M_c) \equiv \sum_{i=1}^N \frac{(\phi_{M,i}(M_c) - \phi_{D,i})^2}{\sigma_{D,i}^2} \quad (1)$$

Here, i runs over the N observed magnitude bins; $\phi_{M,i}(M_c)$ and $\phi_{D,i}$ are the modelled and observed LFs in the i th magnitude bin, respectively, while $\sigma_{D,i}$ is the reported uncertainty in the i th magnitude bin. As the reported errors are slightly asymmetric, we use the (upper, lower) error if the model is (above, below) the data. With no tuning of parameters, $\chi^2(M_c = 0) = 9.91$ for 13 data points, reinforcing the visual impression that the baseline model is in good agreement with the data.

Having computed $\chi^2(M_c)$, we follow Livermore et al. (2016) by using the Bayesian Information Criterion (BIC) to ask how strongly a given minimum halo mass is ruled out. First, we compute the BIC for the base model, which is the simulation itself with no adjustable parameters; this is just $\chi^2(M_c = 0)$. Next, we vary the cutoff halo mass M_c and compute the BIC

$$\text{BIC}(M_c) = \chi^2(M_c) + k \ln(N) \quad (2)$$

where $k = 1$ is the number of parameters in the adjustable model and N is the number of magnitude bins for which Livermore et al. (2016) report a LF measurement. We then compute $\Delta\text{BIC}(M_c) \equiv \text{BIC}(M_c) - \text{BIC}(0)$. Kass & Raftery (1995) find that $\Delta\text{BIC} > (2, 6, 10)$ indicates (positive, strong, very strong) evidence against the more adjustable model.

At $z = 6$, we find that $\Delta\text{BIC} > 2$ for all adjustable models simply because $N > 10$. However, it exceeds (6,10) for $\log(M_c) > (9.5, 9.7)$, indicating strong evidence against significant suppression of star formation in halos less massive than $10^{9.5} M_{\odot}$ (Figure 3). Repeating this analysis at $z = 7$, we find that ΔBIC is above (6,10) for $\log(M_c) = (9.75, 9.95)$. Models in which $M_{\min} \geq 10^{10} M_{\odot}$ are therefore ruled out for

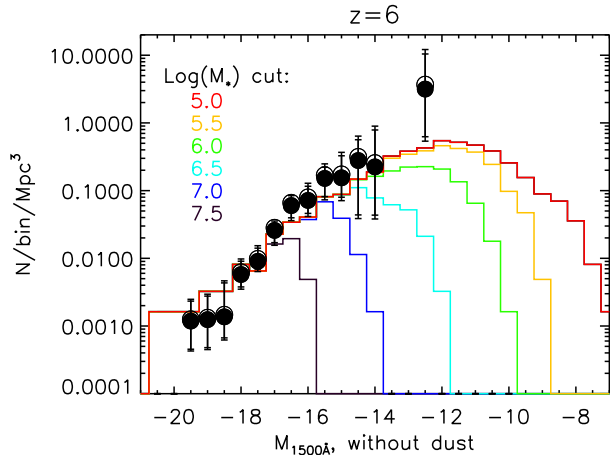


Figure 4. The simulated and observed luminosity functions at $z = 6$. The red curve shows the LF if no simulated galaxies are omitted; it is the same as the red curve in Figure 2. Analogously to Figure 2, increasing the minimum stellar mass removes successively brighter galaxies, weakening the agreement with observations.

$z = 6-7$. At $z = 8$, the shallower nature of the data leads to a weaker constraint: $\Delta\text{BIC} > 6$ for $\log(M_c) > 10.25$, and it never exceeds 10. We have separately evaluated the impact of satellites by ignoring them entirely, finding that the inferred threshold halo mass decreases by less than a factor of two. For simplicity, however, we report results in the case where satellite systems are included.

A related question regards the minimum stellar mass that is currently probed by Frontier Fields data: Are they sensitive to analogues to the progenitors of Local Group dwarf galaxies? The answer depends both on the minimum stellar mass that the observations probe, and on the amount of subsequent growth that can be expected from $z = 6 \rightarrow 0$. We address this question using the same approach as before: by removing galaxies whose total formed stellar mass exceeds a threshold and computing the ΔBIC that relates the predicted luminosity functions with and without the threshold. Throughout this analysis, we adopt the total stellar mass formed rather than the mass that remains in stars in order to facilitate comparison with Weisz et al. (2014a).

As we show in Figure 4, the level of agreement with observations at $z = 6$ begins to weaken once the minimum stellar mass is increased above $10^6 M_\odot$. Quantifying this impression via the ΔBIC analysis, we find that models in which observations do not probe down to stellar masses of $8.1 \times 10^6 M_\odot$ at $z = 6$ are strongly disfavored (Figure 5). The minimum stellar mass is somewhat larger at higher redshifts, but even at $z = 8$ we find that current observations probe down to stellar masses of $3.2 \times 10^7 M_\odot$.

To place this scale in context, we have used Weisz et al. (2014a) to compute the total stellar mass formed in various local group dwarfs by $z = 4.8$. These range from $\sim 10^3 - 10^7 M_\odot$, with the implication that some of them were already massive enough at $z = 5$ that the Frontier Fields may be identifying analogues to their progenitors at $z \geq 6$. To emphasize this overlap, we indicate the total stellar mass formed in three representative dwarfs by $z = 4.8$ in Figure 5. The progenitors of M32 and Pegasus would very likely have

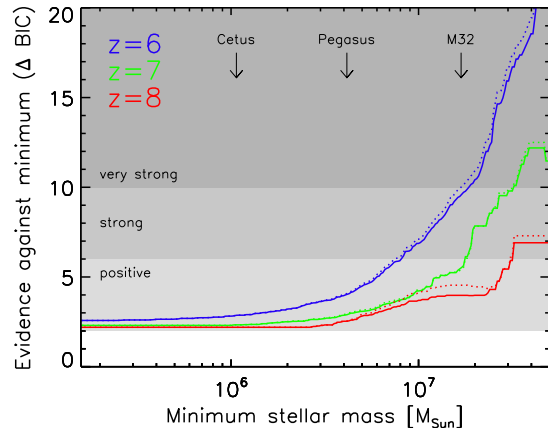


Figure 5. $\Delta\text{BIC}(M_*)$ versus M_* ; (blue, green, red) indicate the constraints at $z = (6, 7, 8)$; the size of the Eddington Bias correction is indicated as in Figure 3. The data, when compared with our model, provide strong evidence that observations probe at least down to stellar masses of $6 \times 10^6 M_\odot$ at $z = 6$, with higher minima at higher redshifts. The arrows label the total stellar masses formed in three local group dwarf galaxies by $z = 5$ (Weisz et al. 2014a). Current data likely probe the progenitors of massive dwarfs such as Pegasus and M32, but not smaller ones such as Cetus.

been observable, while that of Cetus would not. Deeper *HST* data will be required to constrain the amount of star formation that occurred in local dwarfs prior to $z = 4.8$, and will test the association between local group and Frontier Fields dwarfs in more detail.

The Livermore et al. (2016) LF measurements may be subject to Eddington bias; that is, the tendency to overestimate the proportion of rarer, brighter objects owing to contamination by more common, fainter objects that scatter into brighter bins. Livermore et al. (2016) account for this consistently when they fit Schechter functions to their measurements, but the measurements themselves are uncorrected. In order to account for this, we compute the ratio of the Schechter functions derived both with and without the Eddington bias correction⁴ and take the ratio of these as a correction factor. The correction varies with magnitude but is in the range of 0.8–0.9 for $z = 6-7$ and 0.5–0.9 for $z = 8$. We then derive the ΔBIC curve both with (dashed) and without (solid) the correction. Correcting only the measurements in this way (while leaving the reported uncertainties unchanged) lowers the LF amplitude, increasing the limit on M_{min} by 0.05–0.1 dex. Intuitively, if there are fewer galaxies observed, then we may remove fewer halos from the model before it conflicts with data. However, multiplying the uncertainties by the same correction factor makes $\chi^2(M_c)$ more sensitive to M_c , moving the ΔBIC curve to lower halo masses by a similar amount. The end result is a nearly-complete cancellation between the two corrections (compare the dashed and solid curves). We conclude that Eddington bias is not a major uncertainty in the minimum

⁴ The uncorrected fits are not published

halo and stellar mass of the systems that Livermore et al. (2016) identify.

In summary, the Livermore et al. (2016) data provide strong evidence against significant suppression of star formation in halos less massive than $10^{10.25} M_{\odot}$ throughout the range $z = 6-8$, with the strongest constraint coming from $z = 6$, where the data require star formation in halos at least as massive as $10^{9.5} M_{\odot}$. At the same time, our model suggests that the faintest directly-detected galaxies are comparable in stellar mass to the progenitors of Local Group dwarfs. This supports the exciting possibility of using reionization-epoch observations to study the early stages of their growth, just as it supports using the local group to draw inferences regarding the galaxies that drove reionization (for example, Boylan-Kolchin et al. 2014).

4 DISCUSSION

The purpose of this study is, in essence, to invoke the relation shown in Figure 1 (and its analogues at higher redshifts) in order to constrain M_{\min} from the observed UV LF. Our analysis shows that current observations already exert pressure on some previous treatments for star formation. For example, we find that star formation must be relatively unsuppressed in halos down to $3.1 \times 10^9 M_{\odot}$ at $z = 6$, whereas the fiducial metallicity-based H_2 model of Krumholz & Dekel (2012) predicts $\approx 80\%$ suppression at this mass scale (their Figure 8). Our results are also in conflict with the accretion-floor model of Bouché et al. (2010): if halos below $10^{11} M_{\odot}$ do not form stars, then galaxies must populate halos in a very different way than arises in hydrodynamic simulations (that is, Figure 1) in order to match the Livermore et al. (2016) measurements. Of course, the Bouché et al. (2010) model was forwarded as an interpretation of observations at $z \leq 6$, hence a more convincing test would be to repeat our analysis using the observed UV LF at lower redshifts. For the present, we therefore limit ourselves to the conclusion that an accretion floor at $10^{11} M_{\odot}$ does not apply at $z > 6$. This agrees with Behroozi et al. (2013), whose analysis of the stellar mass - halo mass relation likewise indicates robust star formation in $10^{10} M_{\odot}$ halos out to $z = 8$.

An obvious improvement over our study would be to *test* the prediction presented in Figure 1. In order to motivate the need for such a test, we compare our analysis to two previous efforts. Muñoz & Loeb (2011) constructed a semi-analytical model and used it to analyze the shallower observations that were available at the time ($M_{UV} \leq -18$). In their entirely complementary model, halos are assumed to condense their gas into a star-forming disk whenever there is a merger, after which the condensed gas forms into stars. They fitted simultaneously for the luminosity amplitude L_{10} (that is, the luminosity $\log(L_{1500}/\text{erg s}^{-1}\text{Hz}^{-1})$ within $10^{10} M_{\odot}$ halos), and for M_{\min} (m_{supp} in their notation), and found that $M_{\min} \leq 10^{9.5} M_{\odot}$ at $z = 6$ (we will compare with their results only at $z = 6$; similar results occur at $z = 7$ and $z = 8$). In other words, for an observed luminosity function that probes $100\times$ shallower than Livermore et al. (2016), they derived roughly the same M_{\min} as we do. It is reasonable to assume that, were they to confront their model with the most recent constraints, the inferred M_{\min} would

be much lower than ours. This discrepancy reveals a very significant theoretical uncertainty.

The fact that both models match the observed LF’s normalization despite this remarkable discrepancy owes to a cancellation between two effects. First, their derived normalization $L_{10} = 27.2$ is nearly $10\times$ larger than our model, which predicts $L_{10} = 26.3$ (Figure 1), corresponding to a much lower star formation efficiency. Second, their model predicts highly bursty star formation histories: For their fiducial model, the “active fraction” of $10^{10} M_{\odot}$ halos is $< 50\%$. Additionally, their model assumes that star formation in satellite halos stops whenever there is a major merger. This contrasts with our model, in which star formation is generally smooth (Finlator et al. 2011) and satellites constitute a significant fraction of the observable population (Figure 1). Together, these differences increase the predicted characteristic luminosity at a given halo mass with respect to our model.

More recently, Castellano et al. (2016) (see also Yue et al. 2014, 2016) confronted a different semi-analytic model with Frontier Fields measurements that probed down to $M_{UV} = -15$ and inferred that the threshold circular velocity must be below 50 km s^{-1} , corresponding to a halo mass threshold of $\log(M_c/M_{\odot}) = 9.3$. Given that their input LF is 2–3 magnitudes shallower than ours, the result that the inferred halo mass threshold is similar once again implies a discrepancy in the underlying physics. It is likely that, as before, tradeoffs between the unknown burstiness and star formation efficiency of high-redshift galaxies are to blame.

The need for observations that can distinguish between these models is clear. For example, *JWST* will enable measurements of the relationship between complementary observables such as UV luminosity, continuum slope, stellar mass, and $H\alpha$ luminosity, which will probe the underlying level of burstiness. In the nearer term, comparison with clustering measurements may already be able to distinguish between the models; however, this is beyond the scope of the current study. For the present, it is most noteworthy that, in all three analyses, observations forbid star formation to be suppressed in halos above $\log(M_c/M_{\odot}) = 9.5$.

The uncertainties inherent in using galaxy formation models to interpret the UV LF may be mitigated by invoking observations of long gamma-ray bursts (LGRBs), which are also believed to trace star formation. Wei et al. (2016) recently used a simple model that ties galaxy growth and LGRBs to the evolving dark matter halo mass function to derive M_{\min} from *Swift* observations. At 1σ confidence, they constrain it to be less than $10^{10.5} M_{\odot}$ at $z < 4$ and in the range of $10^{7.7}-10^{11.6} M_{\odot}$ at $4 < z < 5$. These results are consistent with ours, although they apply to lower redshifts.

Finally, we note that there is room for progress in reducing both observational and theoretical uncertainties. On the observational side, the luminosity of the faintest *Hubble Frontier Fields* sources remain uncertain owing to the challenge of measuring faint sources in lensed fields. Additionally, the unknown intrinsic sizes of the lensed sources introduces uncertainty into the observational incompleteness corrections that are needed to compute volume densities. The effect is particularly dramatic for the faintest luminosities (Bouwens et al. 2016). On the theoretical side, resolution limitations may affect our analysis: with our cos-

mology and dynamic range, the minimum stellar mass to which Livermore et al. (2016) probe ($6 \times 10^6 M_\odot$; Figure 5) corresponds to ≈ 52 star particles, whereas we have previously argued that 64 are required for converged predictions of global galaxy properties such as mass and luminosity (Finlator et al. 2006). The host halos, by contrast, are quite well-resolved: the minimum halo mass of $3.1 \times 10^9 M_\odot$ corresponds to 7100 dark matter particles, which is more than sufficient to resolve both the halo’s mass and internal structure (Trenti et al. 2010) as well as its gas accretion history (Naoz et al. 2009). Hence while we do not believe that resolution limitations are severe, at present they limit our ability to comment in more detail on the nature of the faintest currently-observed galaxies.

5 SUMMARY

We have combined predictions from a cosmological radiation hydrodynamic simulation with observations of the UV LF at $z = 6-8$ in order to constrain the minimum mass dark matter halo in which star formation is unsuppressed. We find that recent observations require vigorous star formation in halos at least as massive as $(3.1, 5.6, 10.5) \times 10^9 M_\odot$ at $z = (6, 7, 8)$, ruling out models in which significant suppression is expected in halos as massive as $10^{10} M_\odot$. Likewise, we find that these observations probe objects with total formed stellar masses (at the observed epoch) in the range $8-32 \times 10^6 M_\odot$. This overlaps with the range of inferred stellar masses of local group dwarfs at $z = 4.8$, indicating that the Frontier Fields may well contain fairly direct insights into the early growth histories of local dwarfs. Lingering degeneracies between unknowns such as the duty cycle of star formation and the normalization of the $M_{UV}-M_h$ relation indicate that future work involving galaxy colors and clustering measurements are required in order to constrain models further.

ACKNOWLEDGEMENTS

We thank our colleagues at NMSU for helpful conversations and input and R. Bouwens for comments on an early draft. We also thank the referee for comments that improved the draft. We are indebted to V. Springel for making GADGET-3 available to our group, and to P. Hopkins for kindly sharing his SPH module. Our simulation was run on GARDAR, a joint Nordic supercomputing facility in Iceland. KF thanks the Danish National Research Foundation for funding the Dark Cosmology Centre. EZ acknowledges research funding from the Swedish Research Council, the Wenner-Gren Foundations and the Swedish National Space Board.

REFERENCES

- Alvarez, M. A., Finlator, K., & Trenti, M. 2012, ApJL, 759, L38
- Atek, H., Richard, J., Jauzac, M., et al. 2015, ApJ, 814, 69
- Heckman, T. M., Leitherer, C., & Overzier, R. A. 2014, Science, 346, 216
- Behroozi, P. S., Wechsler, R. H., & Conroy, C. 2013, ApJ, 770, 57
- Bouché, N., Dekel, A., Genzel, R., et al. 2010, ApJ, 718, 1001
- Bouwens, R. J., Illingworth, G. D., Oesch, P. A., et al. 2014, ApJ, 793, 115
- Bouwens, R. J., Illingworth, G. D., Oesch, P. A., et al. 2016, arXiv:1608.00966
- Boylan-Kolchin, M., Bullock, J. S., & Kaplinghat, M. 2011, MNRAS, 415, L40
- Boylan-Kolchin, M., Bullock, J. S., & Garrison-Kimmel, S. 2014, MNRAS, 443, L44
- Boylan-Kolchin, M., Weisz, D. R., Johnson, B. D., et al. 2015, MNRAS, 453, 1503
- Calzetti, D., Armus, L., Bohlin, R. C., et al. 2000, ApJ, 533, 682
- Castellano, M., Yue, B., Ferrara, A., et al. 2016, ApJL, 823, L40
- Christensen, C. R., Davé, R., Governato, F., et al. 2016, ApJ, 824, 57
- Conroy, C., Gunn, J. E., & White, M. 2009, ApJ, 699, 486
- Davé, R., Katz, N., Oppenheimer, B. D., Kollmeier, J. A., & Weinberg, D. H. 2013, MNRAS, 434, 2645
- Dekel, A., & Silk, J. 1986, ApJ, 303, 39
- Eisenstein, D. J., & Hu, W. 1999, ApJ, 511, 5
- Efstathiou, G. 1992, MNRAS, 256, 43P
- Finkelstein, S. L., Papovich, C., Ryan, R. E., et al. 2012, ApJ, 758, 93
- Finkelstein, S. L., *in prep*
- Finlator, K., Davé, R., Papovich, C., & Hernquist, L. 2006, ApJ, 639, 672
- Finlator, K., Davé, R., Özel, F. 2011, ApJ, 743, 169
- Finlator, K., Oh, S. P., Özel, F., & Davé, R. 2012, MNRAS, 427, 2464
- Finlator, K., Thompson, R., Huang, S., et al. 2015, MNRAS, 447, 2526
- Finlator, K., Oppenheimer, B. D., Davé, R., et al. 2016, MNRAS, 459, 2299
- Gnedin, N. Y. 2000, ApJ, 542, 535
- Heckman, T. M. 2002, Extragalactic Gas at Low Redshift, 254, 292
- Murray, S. G., Power, C., & Robotham, A. S. G. 2013, Astronomy and Computing, 3, 23
- Iliev, I. T., Mellema, G., Shapiro, P. R., & Pen, U.-L. 2007, MNRAS, 376, 534
- Ishigaki, M., Kawamata, R., Ouchi, M., et al. 2015, ApJ, 799, 12
- Ishigaki, M., Ouchi, M., & Harikane, Y. 2016, ApJ, 822, 5
- Jaacks, J., Thompson, R., & Nagamine, K. 2013, ApJ, 766, 94
- Kass, R. E., Raftery, A. E. 1995, Journ. American Sta. Assoc., 90, 773
- Klypin, A., Kravtsov, A. V., Valenzuela, O., & Prada, F. 1999, ApJ, 522, 82
- Kuhlen, M., Krumholz, M. R., Madau, P., Smith, B. D., & Wise, J. 2012, ApJ, 749, 36
- Kuhlen, M., & Faucher-Giguère, C.-A. 2012, MNRAS, 423, 862
- Krumholz, M. R., & Dekel, A. 2012, ApJ, 753, 16
- Laporte, N., Infante, L., Troncoso Iribarren, P., et al. 2016, ApJ, 820, 98
- Ma, X., Kasen, D., Hopkins, P. F., et al. 2015, MNRAS, 453, 960
- Mesinger, A., & Dijkstra, M. 2008, MNRAS, 390, 1071

8 *The Minimum Mass for Star Formation at $z = 6-8$*

- Murray, N., Quataert, E., & Thompson, T. A. 2005, *ApJ*, 618, 569
- Livermore, R. C., Finkelstein, S. L., & Lotz, J. M. 2016, arXiv:1604.06799
- Muñoz, J. A., & Loeb, A. 2011, *ApJ*, 729, 99
- Muratov, A. L., Kereš, D., Faucher-Giguère, C.-A., et al. 2015, *MNRAS*, 454, 2691
- Naoz, S., Barkana, R., & Mesinger, A. 2009, *MNRAS*, 399, 369
- Okamoto, T., Gao, L., & Theuns, T. 2008, *MNRAS*, 390, 920
- Planck Collaboration, Adam, R., Aghanim, N., et al. 2016, arXiv:1605.03507
- Planck Collaboration, Aghanim, N., Ashdown, M., et al. 2016, arXiv:1605.02985
- Quinn, T., Katz, N., & Efstathiou, G. 1996, *MNRAS*, 278, L49
- Robertson, B. E., Furlanetto, S. R., Schneider, E., et al. 2013, *ApJ*, 768, 71
- Shapiro, P. R., Iliev, I. T., & Raga, A. C. 2004, *MNRAS*, 348, 753
- Springel, V., & Hernquist, L. 2003, *MNRAS*, 339, 289
- Springel, V. 2005, *MNRAS*, 364, 1105
- Thoul, A. A., & Weinberg, D. H. 1996, *ApJ*, 465, 608
- Trenti, M., Smith, B. D., Hallman, E. J., Skillman, S. W., & Shull, J. M. 2010, *ApJ*, 711, 1198
- Veilleux, S., Cecil, G., & Bland-Hawthorn, J. 2005, *ARA&A*, 43, 769
- Wei, J.-J., Hao, J.-M., Wu, X.-F., & Yuan, Y.-F. 2016, *Journal of High Energy Astrophysics*, 9, 1
- Weisz, D. R., Johnson, B. D., & Conroy, C. 2014, *ApJL*, 794, L3
- Weisz, D. R., Dolphin, A. E., Skillman, E. D., et al. 2014, *ApJ*, 789, 147
- Wise, J. H., Demchenko, V. G., Halicek, M. T., et al. 2014, *MNRAS*, 442, 2560
- Wong, W. Y., Moss, A., & Scott, D. 2008, *MNRAS*, 386, 1023
- Yue, B., Ferrara, A., Vanzella, E., & Salvaterra, R. 2014, *MNRAS*, 443, L20
- Yue, B., Ferrara, A., & Xu, Y. 2016, arXiv:1604.01314
- Zackrisson, E., Rydberg, C.-E., Schaerer, D., Östlin, G., & Tuli, M. 2011, *ApJ*, 740, 13